Separation of the Rotational Isomers of Tetrakis(*N*-methyl-2-pyridiniumyl)porphyrin and Crystal Structure of α,α,α,β-(Tetrakis(*N*-methyl-2-pyridiniumyl)porphyrin)copper Hexacyanoferrate

Tai Kaufmann, Bernard Shamsai, Roy Song Lu, Robert Bau, and Gordon M. Miskelly*

Department of Chemistry, University of Southern California, Los Angeles, California 90089-0744

Received February 3, 1995[⊗]

The rotational isomers of tetrakis(*N*-methyl-2-pyridiniumyl)porphyrin (M(T(2-NMePy)P^{4+}); M = Zn^{II}, Cu^{II}, and Ni^{II}) have been separated and isolated as stable solids. The ^{1}H NMR resonances of the *N*-methyl groups are diagnostic of the rotational disposition of the neighboring *N*-methylpyridiniumyl groups. The crystal structure of [α,α,α,β-Cu^{II}(H_2O)T(2-NMePy)P][$HFe^{II}(CN)_6$][$H_2Fe^{II}(CN)_6$]$_{0.5}$·15H_2O (R = 8.53%, R_w = 9.25%, $C2/c$, Z = 4, a = 20.756(3) Å, b = 21.311(3) Å, c = 30.109(4) Å, β = 102.79(3)°) shows that the Cu^{II} is five-coordinate with an axial water. The porphyrins are stacked in a regular sandwich array, with the faces having three positive charges bracketing water-rich regions in the structure, while the faces with one positive charge form loose, slipped porphyrin dimers (interporphyrin distance, 3.85 Å). There are two types of protonated ferrocyanide anions—one ($^1/_2$ per porphyrin unit) embedded in the water-poor region and the other (1 per porphyrin unit) forming dimers linked by hydrogen-bonded waters in the water-rich regions of the structure. The positions of several crystal water oxygens suggest that the two types of ferrocyanide units are linked via hydrogen-bonded waters.

Introduction

The detailed understanding of molecular recognition requires simple models to test predictions and provide data on such factors as local dielectrics[1] and the effect of localized charge. The principal long-range interaction between two charged substrates is the electrostatic attraction or repulsion between the charges. While there are very many studies on the interactions between charged ions in solution, there has been much less work on interactions involving fixed arrays of charge as may be found on the surface of a biological molecule.[2] Studies with discrete molecular species will complement and extend studies using micelles,[3,4] adsorbed monolayers,[5] or charged macromolecules.[6]

The rotational isomers of tetrakis(*N*-methyl-2-pyridiniumyl)-porphyrin (H_2T(2-NMePy)P^{4+}),[7] (Figure 1), provide a simple model to probe the local effects of a charge array. These isomers all have the same inductive influence on the porphyrin and metal center but differ in having 2 + 2, 1 + 3, or 0 + 4 charges on each face of the porphyrin. All previous studies of this porphyrin and its metal derivatives have used mixtures of the possible atropisomers,[7−18] although one report showed possible differences in the EPR spectra of the copper(II) isomers[17] and another showed differences in ^{1}H NMR shifts in a mixture of the iron(III) porphyrin isomers.[10] Contrary to previous reports,[16] it is possible to separate the atropisomers and to maintain the pure isomers for extended periods in both solution and the solid state. This paper reports the synthesis and separation of the isomers and provides a crystal structure for the Cu^{II} derivative of the α,α,α,β isomer.

Experimental Section

Pyridine-2-carboxaldehyde and pyrrole were stored in the refrigerator and were distilled rapidly immediately before use. Dimethyl sulfate was distilled from K_2CO_3. *N*-methylimidazole was distilled from KOH pellets. All solvents were AR grade. Ammonium hexafluorophosphate (95%, Aldrich), NaOH, propanoic acid, LiCl, $Zn(OAc)_2$, $Ni(OAc)_2$, $Cu(OAc)_2$ and $K_4Fe(CN)_6$.3H_2O were used as supplied.

Tetrakis(2-*N*-pyridyl)porphyrin (H_2T(2-Py)P) was prepared in a similar fashion to that reported earlier[19] by adding pyrrole and pyridine-2-carboxaldehyde slowly to a refluxing solution of propanoic acid and then leaving the flask at reflux for 40 min. The solution was then allowed to cool and was vacuum distilled until most solvent was removed. The tarry remnant was triturated with dilute aqueous sodium hydroxide or sodium acetate solutions (either manually or using a Bransonic ultrasonic bath) until the residue became a black powder. The suspension was filtered through Celite, and the black solid was washed with water and air-dried at 40−50 °C. The solid was extracted with warm CH_2Cl_2 and was loaded on a short silica gel column. The column was washed with CH_2Cl_2 and then with CH_2Cl_2 containing increasing amounts of acetone (up to 5% v/v). The porphyrin eluted when the acetone concentration was between 3 and 5%. The impure porphyrin was isolated upon reduction of the volume (Rotavap) and trituration with acetone. This product could be purified by a second chromatography step. However, more typically this impure product was used in the subsequent steps.

[⊗] Abstract published in *Advance ACS Abstracts,* September 1, 1995.

(1) Warshel, A. *Computer Modelling of Chemical Reactions in Enzymes and Solutions*; John Wiley and Sons: New York, 1991.
(2) Rodgers, K. K.; Sligar, S. G. *J. Am. Chem. Soc.* **1991**, *113*, 9419.
(3) Stigter, D. *J. Phys. Chem.* **1964**, *68*, 3603.
(4) Beunen, J. A.; Ruckenstein, E. *J. Colloid Interface. Sci.* **1983**, *96*, 469.
(5) Lee, G. U.; Chrisey, L. A.; Colton, R. J. *Science* **1994**, *266*, 771.
(6) *Polyelectrolytes: Science and Technology*; Hara, M., Ed.; Marcel Dekker, Inc.: New York, 1993.
(7) Hambright, P.; Gore, T.; Burton, M. *Inorg. Chem.* **1976**, *15*, 2314.
(8) Reed, R. A.; Rodgers, K. R.; Kushmeider, K.; Spiro, T. G.; Su, Y. O. *Inorg. Chem.* **1990**, *29*, 2881.
(9) Kobayashi, N. *Inorg. Chem.* **1985**, *24*, 3324.
(10) Rodgers, K. R.; Reed, R. A.; Su, Y. O.; Spiro, T. G. *Inorg. Chem.* **1992**, *31*, 2688.
(11) Bell, S. E. J.; Hester, R. E.; Hill, J. N.; Shawcross, D. R.; Lindsay Smith, J. R. *J. Chem. Soc., Faraday Trans.* **1990**, *86*, 4017.
(12) Chen, S.-M.; Sun, P.-J.; Su, Y. O. *J. Electroanal. Chem.* **1990**, *294*, 151.
(13) Liu, M.; Su, Y. O. *J. Chem. Soc., Chem. Commun.* **1994**, 971.
(14) Chen, S.-M.; Su, Y. O. *J. Electroanal. Chem.* **1990**, *280*, 189.
(15) Kalyanasundaram, K. *Inorg. Chem.* **1984**, *23*, 2453.
(16) Iamamoto, Y.; Serra, O. A.; Idemori, Y. M. *J. Inorg. Biochem.* **1994**, *54*, 55.
(17) Dougherty, G.; Pasternack, R. F. *Inorg. Chim. Acta* **1992**, *195*, 95.
(18) Robinson, L. R.; Hambright, P. *Inorg. Chem.* **1992**, *31*, 652.
(19) Hambright, P.; Adeyemo, A.; Shamim, A.; Lemelle, S. *Inorg. Synth.* **1985**, *23*, 55.

0020-1669/95/1334-5073$09.00/0

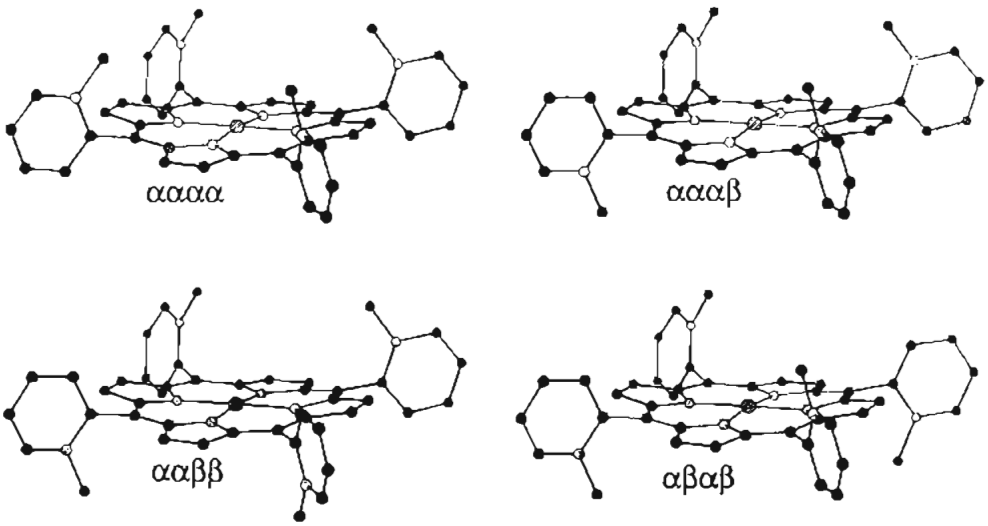

Figure 1. The four atropisomers of M(T(2-NMePy)P^{n+}) showing rotational dispositions of the *N*-methylpyridiniumyl groups and the descriptors used in the text.

$H_2T(2\text{-}NMePy)P^{4+}$ was prepared by heating $H_2T(2\text{-}Py)P$ in dimethyl sulfate at 110 °C.[14] The solution was then pipetted into rapidly stirred ether. The first addition usually caused a gum to form. The gum was dissolved in the minimum amount of methanol, and the addition to ether was repeated until the product was obtained as a green hygroscopic solid. This procedure was found to give higher yields of fully methylated product than reaction with methyl trifluoromethanesulfonate in trimethyl phosphate at 50 °C.[3,4,20,21] Then either this material was used directly to prepare metalloporphyrins, or the less hygroscopic PF_6^- salt was prepared by dissolving the porphyrin in the minimum amount of water and adding excess NH_4PF_6.

Repeated attempts to separate the isomers of the free base porphyrin using thin layer chromatography on silica, alumina, or reversed-phase plates were unsuccessful, as was use of ion exchange columns with aqueous or mixed aqueous–organic eluents. However, ready separation of the isomers of the Ni^{II}, Cu^{II}, or Zn^{II} derivatives was possible using thin layer chromatography (vide infra).

Synthesis of Metal Derivatives. The Cu^{II} and Zn^{II} derivatives were prepared by dissolving the porphyrin in methanol–water or acetone–water mixtures and adding a 10-fold excess of the appropriate metal acetate. Heating at 40–50 °C lead to incorporation of the metal ions. The solutions were then reduced in volume and the metalloporphyrins were precipitated by addition of NH_4PF_6. The Ni^{II} derivative was synthesized using extended reflux in DMF[22] or in H_2O.[23]

Separation of Isomers. The isomers of $Cu^{II}T(2\text{-}NMePy)P^{4+}$ could be separated on analytical (silica gel 60 F_{254}, EM Separations) and preparative (Linear K silica gel 150A, 20 cm x 20 cm x 1000 μm, Whatman) silica gel thin layer chromatography plates. The porphyrin was loaded onto the plates as an acetone solution, and was eluted with 2-butanone–concentrated aqueous ammonia–NH_4PF_6–*n*-butylamine ((10 mL):(1 mL):(0.15 g):(0.1 mL). The Zn^{II} and Ni^{II} derivatives could not be separated with this solvent system but were readily separated by substituting *N*-methylimidazole for *n*-butylamine. Although analytical plates gave clear separations within 12 cm, the preparative chromatography usually required a second plate to obtain isomerically pure material. The fractions containing each isomer were ground with celite and placed in a small column. The porphyrin was eluted either with MeCN–H_2O–saturated aqueous KNO_3 (5:3:2)[24] or with MeCN–H_2O–NH_4PF_6 ((10 mL):(10 mL):(0.15 g)). In the former case the KNO_3 was precipitated by addition of 5 volumes of acetone, the filtrate volume was reduced (Rotavap) until almost all the organic phase was removed then NH_4PF_6 was added and the solution allowed to evaporate slowly until crystallization occurred. The alternative PF_6^--containing eluent from the column was reduced in volume (Rotavap) and then allowed to evaporate until the porphyrin precipitated.

Table 1. Structure Determination Summary

empirical formula	$C_{106}H_{136}Cu_2Fe_3N_{34}O_{32}$	radiation	Cu Kα (graphite monochromator)
MW	2693.1	2θ range (deg)	2.0–102.5
temp	153 K	scan type	ω
space group	*C*2/*c*	scan speed	variable; 8.00–60.00°/min in ω
a (Å)	20.756(3)		
b (Å)	21.311(3)	reflecns collectd	8139
c (Å)	30.109(4)	independ reflecns	6875 (R_{int} = 2.48%)
β (deg)	102.79(3)	obsd reflecns	4770 ($F > 5.0\sigma(F)$)
volume (Å^3)	12988(3)	final *R* indices (obsd data)	R = 8.53%, R_w = 9.25%
Z	4		

X-ray Structure. The PF_6^- salts of these porphyrins readily form microcrystals upon evaporation of acetone–water solutions, but X-ray quality crystals could not be formed even with slow evaporation or use of acetonitrile or 2-butanone instead of acetone. A sample of the Cu^{II} derivative of the α,α,α,β isomer was crystallized with ferrocyanide as follows. $K_4Fe(CN)_6{\cdot}3H_2O$ was dissolved in dilute HNO_3, and diethyl ether was added dropwise until a white precipitate formed.[25] The precipitate was filtered and washed with ether; then it was suspended in ether and treated with a slight excess of ethyldiisopropylamine. The pale blue solid obtained was filtered, washed with ether, and air-dried. This material was still acidic. This solid was dissolved in water and placed in the bottom of a 5-mm NMR tube. Acetonitrile was then layered on top of the solution, followed by a solution of the porphyrin in acetonitrile. Slow diffusion of the solutions led to the formation of glossy purple crystals suitable for X-ray analysis. The X-ray crystal structure was solved at the University of Southern California X-ray Crystallographic Center. A crystal (0.40 × 0.30 × 0.30 mm) of $[\alpha,\alpha,\alpha,\beta\text{-}Cu(H_2O)T(2\text{-}NMePy)P][HFe(CN)_6][H_2Fe(CN)_6]_{0.5}{\cdot}15H_2O$ was sealed in grease, mounted on a Siemens P4/RA automatic diffractometer, and analyzed using Cu Kα radiation monochromatized by a highly oriented graphite crystal. Data were collected at low temperature (153 K) to avoid solvent loss. Four standard reflections, measured after every 97 data points were collected, showed no variation during data collection. Final cell constants, as well as other information pertaining to data collection and refinement, are given in Table 1. All calculations were made using the SHELX system of crystallographic programs.[26] The structure was solved by direct methods,[27] which

(20) Miskelly, G. M.; Webley, W. S.; Clark, C. R.; Buckingham, D. A. *Inorg. Chem.* **1988**, *27*, 3773.
(21) La, T.; Richards, R.; Miskelly, G. M. *Inorg. Chem.* **1994**, *33*, 3159.
(22) Adler, A. D.; Longo, F. R.; Kampas, F.; Kim, J. *J. Inorg. Nucl. Chem.* **1970**, *32*, 2443.
(23) Pasternack, R. F.; Spiro, E. G.; Teach, M. *J. Inorg. Nucl. Chem.* **1974**, *36*, 599.
(24) Elliott, C. M.; Freitag, R. A.; Blaney, D. D. *J. Am. Chem. Soc.* **1985**, *107*, 4647.
(25) Cotton, F. A.; Wilkinson, G. *Advanced Inorganic Chemistry:* 5th ed.; John Wiley and Sons: New York, 1988.
(26) Sheldrick, G. M. SHELX-76. University of Cambridge: Cambridge, U. K., 1976.

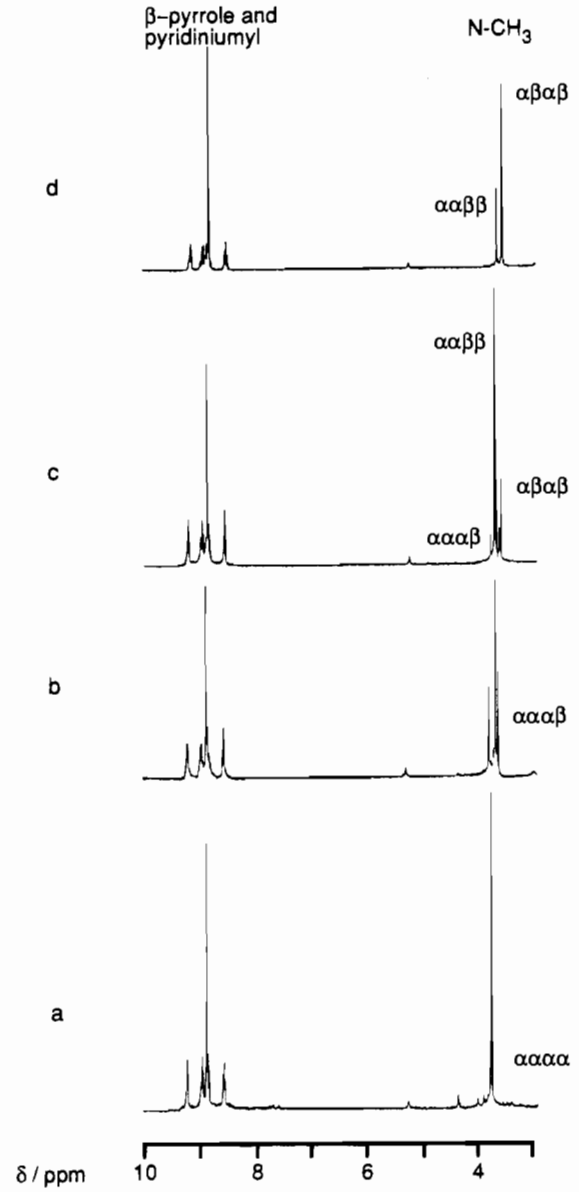

Figure 2. ^{1}H NMR spectra (in CD_3CN) of fractions obtained from a single chromatographic separation of the atropisomers of ZnT(2-NMePy)P^{4+} using the conditions described in the Experimental Section. a−d are the slowest to fastest fractions, respectively.

showed four porphyrin molecules in the unit cell. Calculated hydrogen positions were entered for the porphyrin and constrained to riding motions with fixed isotropic U. Hydrogens were not placed on the solvent water oxygens.

Results and Discussion

The synthetic procedure given above does not necessarily lead to a better yield of the porphyrin H$_2$T(2-NMePy)P^{4+} than those of previous reports, but it does provide more detail than earlier accounts, and gives more tractable products at each stage. The impure H$_2$T(2-Py)P is soluble in acetone but becomes insoluble in this solvent upon purification. Methylation to form H$_2$T(2-NMePy)P^{4+} is straightforward, and leads to an approximately statistical distribution of the four rotational atropisomers. The isomers of free base H$_2$T(2-NMePy)P^{4+} co-eluted under all conditions investigated. However, the atropisomers of the metallated species with Cu^{II}, Ni^{II}, and Zn^{II} could be separated on silica gel using an eluent which contained aqueous ammonia, NH_4PF_6, 2-butanone, and an amine such as 1-butylamine or *N*-methylimidazole. The separation was sensitive to the relative amounts of these components, and substitution of NH_4PF_6 by other salts, or 2-butanone by acetone or acetonitrile, gave inferior separations. The chromatographic separation of the isomers was readily scaled up from analytical to preparative TLC plates. Figure 2 shows ^{1}H NMR spectra of the Zn^{II} derivative after a single separation of 100 mg of the mixed isomers on a 20 × 20 × 0.1 cm plate. The slowest moving band (α,α,α,α) is isomerically pure, the next band (α,α,α,β) is contaminated with about 5% of α,α,β,β, while the next two fractions contained 80% α,α,β,β + 20% α,β,α,β and 30% α,α,β,β + 70% α,β,α,β respectively. The α,α,β,β and α,β,α,β isomers were most difficult to separate, as might be expected given their similar overall structure. Rechromatography of the impure fractions leads to isomerically pure porphyrins. The slowest trimethylated material travels slightly faster than the α,β,α,β tetramethylated band. Attempts to perform the separation with tervalent metals or on chromatography columns were unsuccessful. In addition, attempts to enrich the initial mixture in either the α,α,α,α isomer (by heating acetonitrile solutions in contact with silica gel)[28,29] or the α,β,α,β isomer (by heating in 1-napthol,[30] or by irradiation[31]) have been unsuccessful.

Table 2. ^{1}H NMR Chemical Shifts of [ZnT(2-NMePy)P]$^{4+}$ Pyridiniumyl Methyl Groups in CD_3CN

no. of neighboring methyl groups on same face	isomer	δ (ppm)
0	α,β,α,β	3.870
	α,α,α,β	3.876
1	α,α,β,β	3.930
	α,α,α,β	3.927
2	α,α,α,α	3.990
	α,α,α,β	3.986

The products obtained upon chromatography are stable toward atropisomerization over extended periods, both in the solid state and in solution. For example, the NMR tube containing the acetonitrile solution of α,β,α,β-ZnT(2-NMePy)P^{4+} shown in Figure 2d was left at room temperature for 30 days. After this time the fraction of α,α,α,β (the most dominant isomer at thermal equilibrium and the isomer intermediate between all others[31]) in the solution was <2%. The ^{1}H NMR chemical shifts for the *N*-methyl hydrogens in the zinc derivative in acetonitrile are given in Table 2. The three isomers α,α,α,α, α,β,α,β and α,α,β,β (C_{4v}, D_{2d} and C_{2h} averaged symmetries, respectively) show only one methyl resonance, while the α,α,α,β isomer (C_s symmetry) shows three methyl resonances with intensities 1:2:1. The chemical shifts are mainly dependent on the spatial arrangement of the adjacent charges and are almost independent of the orientation of the opposite methyl group. Thus, the methyl group resonances fall in three regions, with methyls with two cis neighboring methyls resonating at 3.98−4.00 ppm, with one cis neighbor at 3.92−3.93 ppm, and with no cis neighboring methyls at 3.87−3.88 ppm. The β-pyrrole signal is also expected to show some variation, but the observed shifts were less than 0.02 ppm, and the signals could not be differentiated using a 360-MHz NMR spectrometer.

The crystal structure confirmed our assignment of the second-slowest band as the α,α,α,β isomer. The band assignments had

(27) Sheldrick, G. M. SHELX-86. University of Gottingen: Gottingen, Germany, 1986.
(28) Elliott, C. M. *Anal. Chem.* **1980**, *52*, 666.
(29) Lindsey, J. *J. Org. Chem.* **1980**, *45*, 5215.
(30) Rose, E.; Quelquejeu, M.; Pochet, C.; Julien, N.; Kossanyi, A.; Hamon, L. *J. Org. Chem.* **1993**, *58*, 5030.
(31) Freitag, R. A.; Whitten, D. G. *J. Phys. Chem.* **1983**, *87*, 3918.

Table 3. Atomic Coordinates ($\times 10^4$) and Equivalent Isotropic Displacement Coefficients ($Å^2 \times 10^3$)[a]

	x	y	z	U(eq)		x	y	z	U(eq)
Cu(1)	4824(1)	408(1)	5910(1)	34(1)	C(1B)	2756(5)	184(5)	6430(3)	33(2)
Fe(1)	2865(1)	3469(1)	7037(1)	57(1)	C(2B)	2156(5)	165(6)	6136(4)	48(3)
Fe(2)	10000	0	5000	32(1)	C(3B)	1582(6)	105(6)	6293(4)	58(3)
N(1)	5385(4)	1128(4)	5800(3)	38(2)	C(4B)	1615(6)	33(6)	6736(4)	56(3)
N(2)	4194(4)	995(4)	6110(3)	29(2)	C(5B)	2203(6)	50(7)	7028(4)	64(3)
N(3)	4259(4)	−316(4)	6013(3)	32(2)	C(6B)	3401(6)	132(9)	7207(4)	88(3)
N(4)	5384(4)	−180(4)	5638(3)	47(2)	C(1C)	4903(7)	−1868(6)	5725(5)	65(3)
N(1A)	4526(4)	3107(4)	5925(3)	40(2)	C(2C)	4587(11)	−2198(7)	5372(6)	113(3)
N(1B)	2774(4)	127(5)	6878(3)	50(2)	C(3C)	5318(12)	−2824(8)	6062(11)	189(3)
N(1C)	5279(7)	−2180(6)	6080(7)	128(3)	C(4C)	5016(11)	−3146(7)	5700(9)	138(3)
N(1D)	7433(5)	439(5)	5703(4)	61(2)	C(5C)	4647(11)	−2844(8)	5357(7)	130(3)
N(1X)	1667(5)	4374(5)	6794(4)	67(3)	C(6C)	5626(12)	−1854(10)	6493(11)	248(3)
N(2X)	3045(6)	3589(7)	6052(4)	96(3)	C(1Y)	9803(5)	210(5)	5575(4)	37(2)
N(3X)	3846(6)	4583(7)	7290(5)	100(3)	C(2Y)	10769(6)	521(5)	5147(5)	45(2)
N(4X)	2658(8)	3398(7)	8028(5)	121(3)	C(3Y)	10404(5)	−701(5)	5300(4)	32(2)
N(5X)	2002(7)	2321(7)	6707(7)	139(3)	C(1D)	6897(6)	606(5)	5395(5)	52(3)
N(6X)	3982(7)	2504(7)	7323(4)	111(3)	C(2D)	6942(6)	816(6)	4972(4)	58(3)
N(1Y)	9685(5)	323(4)	5923(3)	54(2)	C(3D)	7567(6)	859(6)	4868(5)	61(3)
N(2Y)	11235(5)	824(5)	5226(4)	68(2)	C(4D)	8116(5)	690(6)	5197(5)	65(3)
N(3Y)	10778(5)	−1122(4)	5495(3)	48(2)	C(5D)	8036(7)	468(7)	5606(5)	80(3)
C(1)	5884(6)	2092(5)	5869(4)	54(3)	C(6D)	7385(8)	215(10)	6159(6)	120(3)
C(2)	5322(5)	1743(5)	5922(3)	33(2)	C(1X)	2106(6)	4052(6)	6880(4)	53(3)
C(3)	4799(5)	1992(5)	6076(3)	31(2)	C(2X)	2979(6)	3539(7)	6427(5)	66(3)
C(4)	4262(5)	1643(5)	6156(3)	32(2)	C(3X)	3477(7)	4168(7)	7198(5)	70(3)
C(5)	3703(5)	1903(5)	6303(4)	40(2)	C(4X)	2728(7)	3430(7)	7643(5)	78(3)
C(6)	3312(5)	1425(5)	6351(4)	37(2)	C(5X)	2313(7)	2750(7)	6835(6)	93(3)
C(7)	3619(5)	860(5)	6235(3)	34(2)	C(6X)	3579(7)	2878(8)	7207(5)	79(3)
C(8)	3388(5)	250(5)	6282(3)	30(2)	O(1)	5637(4)	253(5)	6666(3)	81(2)
C(9)	3700(5)	−290(5)	6191(3)	32(2)	O(2)	3012(4)	3342(4)	9017(3)	60(2)
C(10)	3490(5)	−915(5)	6266(4)	39(2)	O(3)	0	3333(7)	2500	84(3)
C(11)	4378(5)	−939(5)	5965(4)	39(2)	O(4)	2676(6)	2450(6)	482(4)	122(3)
C(13)	4869(6)	−1172(5)	5763(5)	52(3)	O(5)	2643(8)	4044(8)	5147(6)	170(4)
C(14)	5319(6)	−826(5)	5597(5)	61(3)	O(6)	3362(8)	2767(8)	4340(6)	181(4)
C(15)	5819(8)	−1065(6)	5374(7)	99(3)	O(7)	3665(9)	1385(8)	8055(6)	190(4)
C(16)	6200(8)	−581(6)	5307(6)	93(3)	O(8)	0	251(12)	7500	198(5)
C(17)	5947(6)	−34(6)	5488(5)	60(3)	O(9)	5095(13)	355(12)	2793(8)	139(4)
C(18)	6227(6)	556(5)	5515(4)	51(3)	O(10)	2419(10)	3074(10)	1829(7)	239(4)
C(19)	5978(5)	1096(5)	5672(4)	44(2)	O(11)	1815(9)	1817(9)	8854(7)	218(4)
C(20)	6284(6)	1698(5)	5710(5)	55(3)	O(12)	2881(12)	2052(11)	4859(8)	283(5)
C(1A)	4830(5)	2664(5)	6222(4)	36(2)	O(13)	3957(11)	2122(10)	2261(7)	249(4)
C(2A)	5175(7)	2851(5)	6638(4)	61(3)	O(14)	5070(9)	475(9)	7760(6)	83(4)
C(3A)	5195(7)	3478(6)	6755(4)	69(3)	O(15)	4946(13)	4000(12)	3231(9)	302(5)
C(4A)	4875(6)	3912(5)	6453(4)	50(3)	O(16)	4321(18)	−2789(18)	6615(13)	444(5)
C(5A)	4550(6)	3716(5)	6044(4)	47(3)	O(17)	3807(22)	3356(22)	2736(16)	556(5)
C(6A)	4163(8)	2918(6)	5462(4)	74(3)	O(18)	4045(17)	4105(16)	1557(12)	404(5)

[a] Atoms Fe(2), O(3), O(8), O(9), and O(14) have populations of 50%. All other atoms have populations of 100%.

been made on the basis of the common tetrakis(ortho-substituted phenyl)porphyrin elution orders[28,29] and on the intensities (ca. 1:4:2:1 from bottom to top) expected for a statistical distribution of the isomers.[31] The structure of α,α,α,β-[$Cu^{II}(H_2O)$T(2-NMePy)P][$HFe(CN)_6$][$H_2Fe(CN)_6$]$_{0.5}$·$15H_2O$ is shown in Figures 3−5. Table 3 gives atomic coordinates and isotropic displacement coefficients, and Tables 4 and 5 give selected bond distances and angles. The view of the porphyrin shown in Figure 3 clearly shows the disposition of the methyl groups. Inspection of the electron density map at the end of the refinement did not reveal any significant electron density at the other ortho positions to suggest disorder or atropisomerization. The copper is five-coordinate, with a water located on the side with three methylpyridiniumyl groups, with a Cu−O bond distance of at 2.53 Å. This distance is typical for a water molecule located at the axial (elongated) position of copper(II) in octahedral complexes. This axial water is slightly off-center toward the methyl groups, and this may be due to the effect of the proximate charges. This is the first example of a solid-state structure of a copper porphyrin in which the copper has an axial ligand. The presence of an axial ligand can be ascribed to the water-rich region above the porphyrin plane and also to the electron-withdrawing nature of the *N*-methyl-2-pyridiniumyl

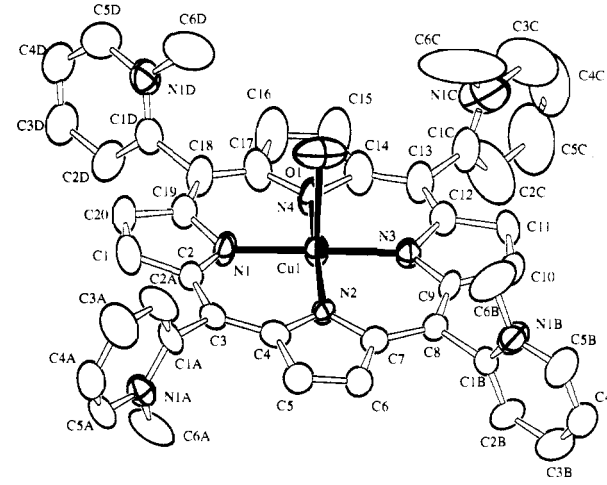

Figure 3. ORTEP diagram of [α,α,α,β-Cu(H_2O)T(2-NMePy)P^{4+}] showing disposition of methyl gruops and axial water and the atom numbering for the porphyrin. Ellipsoids are drawn at 50% probabilities.

substituents. The porphyrin ring shows a slight saddle distortion, and this is shown more clearly in Figure 4 , which shows the displacement of the atoms in the porphyrin ring above and below

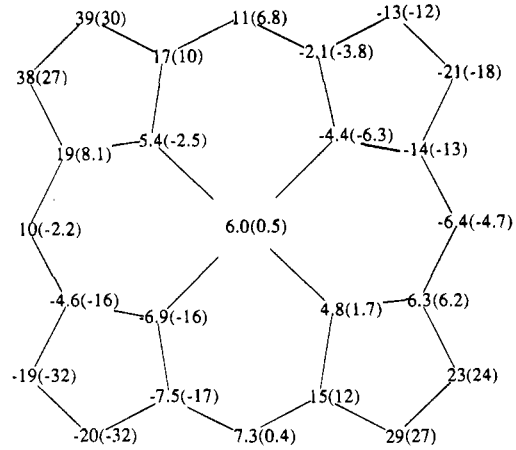

Figure 4. Diagram of the porphyrin core of [α,α,α,β-Cu(H_2O)T(2-NMePy)P^{4+}] showing deviations from the root mean square plane defined by the four core nitrogens and deviations from the root mean square plane defined by the 24-core atoms (in parentheses).

Table 4. Bond Lengths (Å)

Cu(1)−N(1)	1.998(9)	Cu(1)−N(2)	1.997(8)
Cu(1)−N(3)	2.002(8)	Cu(1)−N(4)	2.005(10)
Cu(1)−O(1)	2.538(8)	Fe(1)−C(1X)	1.979(13)
Fe(1)−C(2X)	1.909(15)	Fe(1)−C(3X)	1.948(15)
Fe(1)−C(4X)	1.912(16)	Fe(1)−C(5X)	1.927(15)
Fe(1)−C(6X)	1.927(15)	Fe(2)−C(1Y)	1.919(13)
Fe(2)−C(2Y)	1.914(11)	Fe(2)−C(3Y)	1.921(10)
Fe(2)−C(1YA)	1.919(13)	Fe(2)−C(2YA)	1.914(11)
Fe(2)−C(3YA)	1.921(10)	N(1)−C(2)	1.375(13)
N(1)−C(19)	1.369(15)	N(2)−C(4)	1.393(13)
N(2)−C(7)	1.359(14)	N(3)−C(9)	1.382(14)
N(3)−C(12)	1.363(13)	N(4)−C(14)	1.385(14)
N(4)−C(17)	1.378(17)	N(1A)−C(1A)	1.354(13)
N(1A)−C(5A)	1.345(13)	N(1A)−C(6A)	1.487(15)
N(1B)−C(1B)	1.346(14)	N(1B)−C(5B)	1.371(17)
N(1B)−C(6B)	1.450(14)	N(1C)−C(1C)	1.350(21)
N(1C)−C(3C)	1.376(21)	N(1C)−C(6C)	1.467(32)
N(1D)−C(1D)	1.328(15)	N(1D)−C(5D)	1.348(19)
N(1D)−C(6D)	1.479(22)	N(1X)−C(1X)	1.125(17)
N(2X)−C(2X)	1.173(19)	N(3X)−C(3X)	1.163(20)
N(4X)−C(4X)	1.201(22)	N(5X)−C(5X)	1.136(21)
N(6X)−C(6X)	1.151(21)	N(1Y)−C(1Y)	1.151(17)
N(2Y)−C(2Y)	1.142(15)	N(3Y)−C(3Y)	1.158(13)
C(1)−C(2)	1.421(16)	C(1)−C(20)	1.342(18)
C(2)−C(3)	1.379(15)	C(3)−C(4)	1.403(15)
C(3)−C(1A)	1.495(14)	C(4)−C(5)	1.441(16)
C(5)−C(6)	1.329(15)	C(6)−C(7)	1.442(15)
C(7)−C(8)	1.403(14)	C(8)−C(9)	1.378(14)
C(8)−C(1B)	1.482(15)	C(9)−C(10)	1.435(15)
C(10)−C(11)	1.325(16)	C(11)−C(12)	1.442(16)
C(12)−C(13)	1.391(18)	C(13)−C(14)	1.368(19)
C(13)−C(1C)	1.491(16)	C(14)−C(15)	1.449(24)
C(15)−C(16)	1.342(21)	C(16)−C(17)	1.435(20)
C(17)−C(18)	1.380(16)	C(18)−C(19)	1.387(16)
C(18)−C(1D)	1.516(19)	C(19)−C(20)	1.425(16)
C(1A)−C(2A)	1.359(15)	C(2A)−C(3A)	1.380(17)
C(3A)−C(4A)	1.361(17)	C(4A)−C(5A)	1.335(16)
C(1B)−C(2B)	1.361(14)	C(2B)−C(3B)	1.381(18)
C(3B)−C(4B)	1.330(18)	C(4B)−C(5B)	1.337(16)
C(1C)−C(2C)	1.321(21)	C(2C)−C(5C)	1.385(23)
C(3C)−C(4C)	1.323(34)	C(4C)−C(5C)	1.310(29)
C(1D)−C(2D)	1.373(19)	C(2D)−C(3D)	1.402(19)
C(3D)−C(4D)	1.382(17)	C(4D)−C(5D)	1.365(22)

the root mean square plane. The pyridiniumyl groups show no tilting in directions that would indicate strong intramolecular repulsion between the charged groups.

The porphyrins are arranged in an alternating sandwich lattice of water-rich regions and more hydrophobic regions, Figure 5. The latter regions show interporphyrin distances of 3.85 Å, with the β-carbon positioned over the central metal (r_{Cu-Cu} = 5.95 Å). The interporphyrin distance across the water-rich region is 8.7 Å. The porphyrin face containing the three positive charges and the axial ligand is directed toward the water-rich region. There are two types of ferrocyanide ions in the structure. The first type (one per porphyrin) is in the water-rich regions,

Table 5. Bond Angles (deg)

N(1)−Cu(1)−N(2)	90.8(3)	N(1)−Cu(1)−N(3)	179.4(4)
N(2)−Cu(1)−N(3)	89.5(3)	N(1)−Cu(1)−N(4)	90.0(4)
N(2)−Cu(1)−N(4)	173.3(3)	N(3)−Cu(1)−N(4)	89.7(4)
N(1)−Cu(1)−O(1)	87.2(3)	N(2)−Cu(1)−O(1)	99.2(3)
N(3)−Cu(1)−O(1)	93.3(3)	N(4)−Cu(1)−O(1)	87.5(3)
C(1X)−Fe(1)−C(2X)	89.1(6)	C(1X)−Fe(1)−C(3X)	91.1(6)
C(2X)−Fe(1)−C(3X)	88.1(6)	C(1X)−Fe(1)−C(4X)	88.6(6)
C(2X)−Fe(1)−C(4X)	177.6(6)	C(3X)−Fe(1)−C(4X)	91.2(6)
C(1X)−Fe(1)−C(5X)	92.2(6)	C(2X)−Fe(1)−C(5X)	87.2(7)
C(3X)−Fe(1)−C(5X)	174.2(7)	C(4X)−Fe(1)−C(5X)	93.6(7)
C(1X)−Fe(1)−C(6X)	177.2(6)	C(2X)−Fe(1)−C(6X)	93.1(6)
C(3X)−Fe(1)−C(6X)	90.7(6)	C(4X)−Fe(1)−C(6X)	89.2(6)
C(5X)−Fe(1)−C(6X)	86.1(6)	C(1Y)−Fe(2)−C(2Y)	89.4(5)
C(1Y)−Fe(2)−C(3Y)	87.4(4)	C(2Y)−Fe(2)−C(3Y)	90.7(4)
C(1Y)−Fe(2)−C(1YA)	180.0(1)	C(2Y)−Fe(2)−C(1YA)	90.6(5)
C(3Y)−Fe(2)−C(1YA)	92.6(4)	C(1Y)−Fe(2)−C(2YA)	90.6(5)
C(2Y)−Fe(2)−C(2YA)	180.0(1)	C(3Y)−Fe(2)−C(2YA)	89.3(4)
C(1YA)−Fe(2)−C(2YA)	89.4(5)	C(1Y)−Fe(2)−C(3YA)	92.6(4)
C(2Y)−Fe(2)−C(3YA)	89.3(4)	C(3Y)−Fe(2)−C(3YA)	180.0(1)
C(1YA)−Fe(2)−C(3YA)	87.4(4)	C(2YA)−Fe(2)−C(3YA)	90.7(4)
Cu(1)−N(1)−C(2)	126.5(7)	Cu(1)−N(1)−C(19)	127.0(7)
C(2)−N(1)−C(19)	105.5(8)	Cu(1)−N(2)−C(4)	126.4(7)
Cu(1)−N(2)−C(7)	128.7(7)	C(4)−N(2)−C(7)	105.0(8)
Cu(1)−N(3)−C(9)	126.8(7)	Cu(1)−N(3)−C(12)	127.4(7)
C(9)−N(3)−C(12)	105.5(9)	Cu(1)−N(4)−C(14)	127.0(9)
Cu(1)−N(4)−C(17)	127.1(7)	C(14)−N(4)−C(17)	105.6(10)
C(1A)−N(1A)−C(5A)	120.9(9)	C(1A)−N(1A)−C(6A)	119.7(9)
C(5A)−N(1A)−C(6A)	119.4(9)	C(1B)−N(1B)−C(5B)	120.5(9)
C(1B)−N(1B)−C(6B)	120.3(10)	C(5B)−N(1B)−C(6B)	119.1(10)
C(1C)−N(1C)−C(3C)	119.3(17)	C(1C)−N(1C)−C(6C)	121.7(13)
C(3C)−N(1C)−C(6C)	119.0(18)	C(1D)−N(1D)−C(5D)	120.8(12)
C(1D)−N(1D)−C(6D)	121.2(12)	C(5D)−N(1D)−C(6D)	118.1(11)
C(2)−C(1)−C(20)	107.5(10)	N(1)−C(2)−C(1)	109.9(9)
N(1)−C(2)−C(3)	125.9(9)	C(1)−C(2)−C(3)	124.3(10)
C(2)−C(3)−C(4)	124.6(9)	C(2)−C(3)−C(1A)	118.9(9)
C(4)−C(3)−C(1A)	116.2(10)	N(2)−C(4)−C(3)	125.1(10)
N(2)−C(4)−C(5)	109.9(9)	C(3)−C(4)−C(5)	124.9(9)
C(4)−C(5)−C(6)	107.0(9)	C(5)−C(6)−C(7)	107.5(10)
N(2)−C(7)−C(6)	110.7(9)	N(2)−C(7)−C(8)	124.4(9)
C(6)−C(7)−C(8)	124.7(10)	C(7)−C(8)−C(9)	124.5(10)
C(7)−C(8)−C(1B)	117.6(9)	C(9)−C(8)−C(1B)	117.8(9)
N(3)−C(9)−C(8)	125.7(9)	N(3)−C(9)−C(10)	109.6(9)
C(8)−C(9)−C(10)	124.8(10)	C(9)−C(10)−C(11)	107.7(10)
C(10)−C(11)−C(12)	107.1(9)	N(3)−C(12)−C(11)	110.2(10)
N(3)−C(12)−C(13)	124.1(10)	C(11)−C(12)−C(13)	125.6(10)
C(12)−C(13)−C(14)	126.4(10)	C(12)−C(13)−C(1C)	116.1(11)
C(14)−C(13)−C(1C)	117.5(12)	N(4)−C(14)−C(13)	124.4(12)
N(4)−C(14)−C(15)	108.9(11)	C(13)−C(14)−C(15)	126.6(11)
C(14)−C(15)−C(16)	107.8(13)	C(15)−C(16)−C(17)	106.9(15)
N(4)−C(17)−C(16)	110.4(11)	N(4)−C(17)−C(18)	124.3(12)
C(16)−C(17)−C(18)	125.4(13)	C(17)−C(18)−C(19)	126.3(12)
C(17)−C(18)−C(1D)	116.5(11)	C(19)−C(18)−C(1D)	117.1(10)
N(1)−C(19)−C(18)	124.3(10)	N(1)−C(19)−C(20)	110.2(10)
C(18)−C(19)−C(20)	125.4(11)	C(1)−C(20)−C(19)	106.9(11)
N(1A)−C(1A)−C(3)	119.4(8)	N(1A)−C(1A)−C(2A)	118.5(9)
C(3)−C(1A)−C(2A)	122.0(9)	C(1A)−C(2A)−C(3A)	119.9(11)
C(2A)−C(3A)−C(4A)	120.3(11)	C(3A)−C(4A)−C(5A)	118.5(11)
N(1A)−C(5A)−C(4A)	121.9(10)	N(1B)−C(1B)−C(8)	118.7(8)
N(1B)−C(1B)−C(2B)	117.9(10)	C(8)−C(1B)−C(2B)	123.4(10)
C(1B)−C(2B)−C(3B)	121.0(11)	C(2B)−C(3B)−C(4B)	119.8(10)
C(3B)−C(4B)−C(5B)	119.7(12)	N(1B)−C(5B)−C(4B)	121.0(12)
N(1C)−C(1C)−C(13)	117.3(12)	N(1C)−C(1C)−C(2C)	118.2(12)
C(13)−C(1C)−C(2C)	124.5(12)	C(1C)−C(2C)−C(5C)	121.5(15)
N(1C)−C(3C)−C(4C)	121.9(21)	C(3C)−C(4C)−C(5C)	118.8(16)
C(2C)−C(5C)−C(4C)	120.3(18)	Fe(2)−C(1Y)−N(1Y)	178.6(9)
Fe(2)−C(2Y)−N(2Y)	178.1(10)	Fe(2)−C(3Y)−N(3Y)	177.2(10)
N(1D)−C(1D)−C(18)	119.0(12)	N(1D)−C(1D)−C(2D)	121.1(12)
C(18)−C(1D)−C(2D)	119.9(10)	C(1D)−C(2D)−C(3D)	118.9(11)
C(2D)−C(3D)−C(4D)	118.7(13)	C(3D)−C(4D)−C(5D)	119.4(13)
N(1D)−C(5D)−C(4D)	121.0(12)	Fe(1)−C(1X)−N(1X)	178.5(13)
Fe(1)−C(2X)−N(2X)	179.2(12)	Fe(1)−C(3X)−N(3X)	179.1(11)
Fe(1)−C(4X)−N(4X)	178.3(13)	Fe(1)−C(5X)−N(5X)	177.7(16)
Fe(1)−C(6X)−N(6X)	175.7(15)		

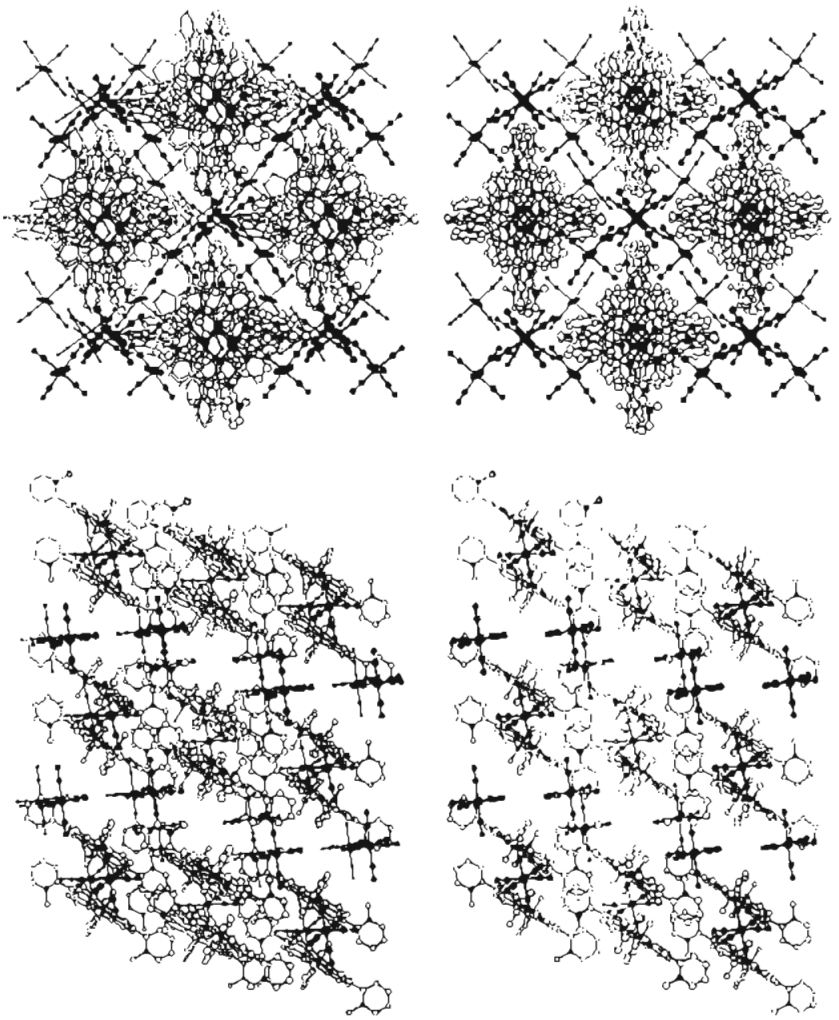

Figure 5. Diagram showing the porphyrins and the anions in [α,α,α,β-Cu(H_2O)T(2-NMePy)P][$HFe(CN)_6$][$H_2Fe(CN)_6$]$_{0.5}$·15H_2O (a, top) down the *c* axis and (b, bottom) down the *a* axis. In each case the right view is along the axis and the left view is rotated by 5°. This diagram was prepared using CSC Chem-3D with atom coordinates entered as fractional crystallographic coordinates. The coordinated and crystal waters have been removed for clarity.

and appears to form a dimer (r_{Fe-Fe} = 8.68 Å) held together by hydrogen bonded water sitting at the intersection of the CN vectors (r_{N-O} = 2.7 Å). The second type of $Fe(CN)_6^{4-}$ (0.5 per porphyrin; situated on an inversion center) is embedded in the hydrophobic region of the structure and provides charge balance for the lone methylpyridinium group on the β face. The structure suggests that the two types of ferrocyanide are loosely hydrogen bonded to intermediate water molecules (r_{N-O} = 2.8–2.9 Å), but the waters are not positioned along the CN vectors. The overall effect is of hydrogen-bonded ribbons of anions running parallel to the c axis in the channels between columns of porphyrin cores, as shown in Figure 5. The molecular formula of the crystal suggests that there are two acidic protons per porphyrin unit from incomplete neutralization of $H_4Fe(CN)_6$ during preparation of the diisopropylethylammonium salt of the anion. The reported acid dissociation constants for $H_4Fe(CN)_6$ show that the coordinated cyanides are the most basic site in the structure (pK_{a3} = 2.2; pK_{a4} = 4.17),[32] suggesting that they will be the site of protonation. However, we were unable to locate the protons. The Fe–C and C–N bond lengths in both types of ferrocyanide are within the range observed previously for protonated[33] and unprotonated[34,35] ferrocyanides.

The lack of orientational disorder of the porphyrins in the crystal can be rationalized by examination of the packing of α,α,α,β structures in a two-dimensional network. Steric and Coulombic forces will be minimized if all the porphyrins in a given layer have the same orientation. Examination of the unit cell suggests that registry between porphyrin layers is maintained by minimization of Coulombic and steric effects (water-poor region) and ion-pairing with the ferrocyanide anions (water-rich region). The crystal lattice also contains a very large amount of lattice water (up to 15 per porphyrin) which occupy a total of 17 sites. These sites vary in the volume and degree of occupancy, with four (including the coordinated water) having significantly smaller thermal ellipsoids than the other sites. The structure was solved assuming full occupancy in all sites except those in special positions, or those placed unreasonably close together (within 2 Å). Waters in those types of positions were assigned occupancies of 0.5.

The crystal structure has a low *R* factor compared to the structures of other water-soluble porphyrin crystals which have been grown in aqueous media.[36,37] This can be attributed to the use of the $Fe(CN)_6^{4-}$ anion, which is not subject to the disorder seen for ClO_4^- ions in the other porphyrin structures.

(32) Jordan, J.; Ewing, G. J. *Inorg. Chem.* **1962**, *1*, 587.
(33) Pierrot, M.; Kern, R.; Weiss, R. *Acta Crystallogr.* **1966**, *20*, 425.
(34) Tullberg, A.; Vannerberg, N.-G. *Acta Chem. Scand.* **1971**, *25*, 343.
(35) Tullberg, A.; Vannerberg, N.-G. *Acta Chem. Scand.* **1974**, *A28*, 551.
(36) Kirner, J. F.; Garofalo, J.; Scheidt, W. R. *Inorg. Nucl. Chem. Lett.* **1975**, *11*, 107.
(37) Ivanca, M. A.; Lappin, A. G.; Scheidt, W. R. *Inorg. Chem.* **1991**, *30*, 711.

In general we have had most success crystallizing water-soluble tetracationic porphyrins either by using nonaqueous recrystallization media or by using anions such as $CF_3SO_3^-$,[38] with lower symmetry than ClO_4^-.

Conclusions

The rotational atropisomers of the Ni^{II}, Cu^{II}, and Zn^{II} derivatives of $H_2T(2\text{-}NMePy)P^{4+}$ have been separated and isolated as solids. Proton NMR and X-ray structural characterizations show that the isomers can be obtained in pure form and that they are stable towards atropisomerization for lengthy periods (>1 month) at room temperature both in the solid state and in solution. The crystal structure of the $\alpha,\alpha,\alpha,\beta$ isomer of $CuT(2\text{-}NMePy)P^{4+}$ shows that the steric effects due to three methylpyridinium groups are not significant impediments to axial coordination at the metal center. The steric effects will be even smaller for the $\alpha,\beta,\alpha,\beta$ and $\alpha,\alpha,\beta,\beta$ isomers. Therefore this system allows examination of the effects of localized charge near a potential binding site. The Zn^{II} derivative can be demetallated to form the free base porphyrin and thereby provides access to other metallo derivatives of the individual isomers. Investigations of the effects of the oriented charges upon ligand binding and reactivity will be reported in subsequent papers.

Acknowledgment. Acknowledgment is made to the Donors of the Petroleum Research Fund, administered by the American Chemical Society, for partial support of this work. This work was also supported by a ZRIF grant from the University of Southern California and a grant from Professor A. B. Burg. The X-ray diffractometer was purchased with funds provided in part by NSF Instrument Grant CHE-92-16167.

Supporting Information Available: Listings of anisotropic displacement coefficients (Table S1) and ligand H atom coordinates and isotropic displacement coefficients (Table S2) (3 pages). Ordering information is given on any current masthead page.

IC950118U

(38) La, T.; Richards, R. A.; Miskelly, G. M. Submitted for publication in *Inorg. Chem.*